PS-wave traveltime difference inversion for S-wave near-surface characterization in the tau-p domain

Raul Cova and Kris Innanen

ABSTRACT

In the processing of P-wave data one important product of computing static corrections is a P-wave near-surface velocity model. This model is usually inverted from the traveltimes of the refracted waves. In the case of converted-wave data, for which S-wave near-surface corrections must be used on the receiver locations, refracted S-waves are usually not available or hard to identify. Here, we propose an inversion approach based on the τ differences obtained by crosscorrelating τ-p receiver gathers from different locations. For this, the structure of the near-surface at a given location must be know. Then, the τ-p receiver gathers are crosscorrelated with the gather obtained at the reference location, and the time lag of the maximum of the crosscorrelation function is picked. These picks along with an initial guess of the depth of the near-surface layer, its S-wave velocity, local dip and velocity of the medium underneath (replacement velocity) are the input to initialize the inversion. An iterative quasi-Newton inversion approach is used in this study. Different data conditions are used to study the robustness of the inversion. Results show that the inversion of the depth of the near-surface layer is very sensitive to the presence of noise in the picks and the lack of large rayparameter values ($p > 0.5$ms/m). Although to a lower degree, inverted velocities were also affected by these conditions. However, inverted dips displayed very stable results under different data conditions. Alternative inversion approaches able to exploit the robustness of the inverted dips must be considered to improve the results provided in this study.

INTRODUCTION

Raypath-consistent interferometric statics were introduced by Henley (2012). As in many interferometric methods, the processing method there proposed is fully data driven. This means that no velocity model is needed to remove the near-surface effects from the data.

However, an S-wave velocity model for the near-surface is of utmost importance for imaging and full waveform inversion (FWI) considering converted wave (PS) data. Due to the lack of S-wave refracted data in the acquisition of most exploration seismic data, S-wave velocity inversion from surface wave data has become into an important approach for characterizing the near-surface. Nevertheless, very dense spatial sampling parameters are required to produce reliable and complete S-wave velocity models by using this method.

Here, we propose a method to compute S-wave near-surface velocities using the information captured by the crosscorrelation functions produced during the interferometric processing of the near-surface effects. This is achieved by inverting the intercept-time (τ) differences between two receiver stations in terms of the rayparameter (p) values. The effects of random noise and limited aperture are also addressed to understand the robustness of this method.

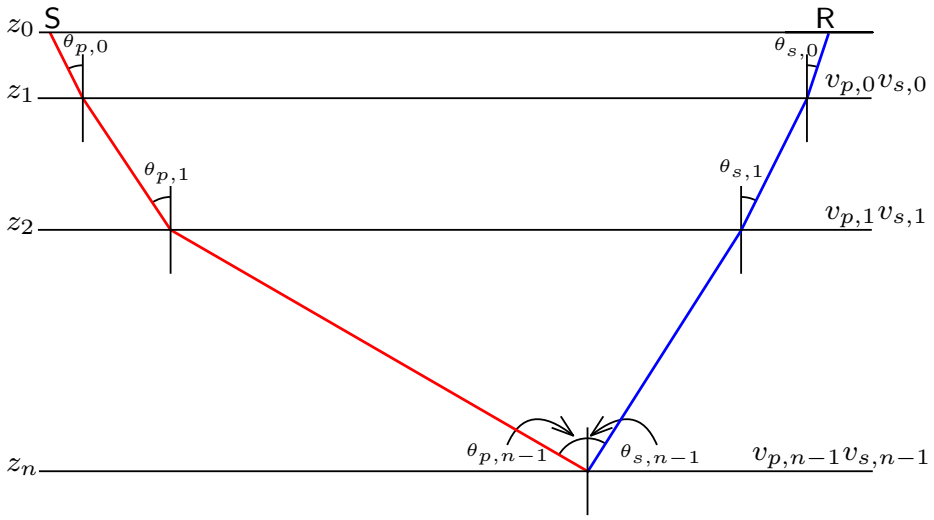

FIG. 1. Schematic representation of a PS-raypath. Despite the asymmetry in the raypath the rayparameter p is constant in a horizontally layered medium.

MODELLING TRAVELTIME DIFFERENCES IN τ-p DOMAIN

In a layered medium, the intercept time τ represents the aggregate vertical slowness-thickness product in equation 1 (Diebold and Stoffa, 1981):

$$\tau = \sum_{i=0}^{n-1} \Delta z_i \left(q_i^d + q_i^u\right) = \tau^d + \tau^u, \tag{1}$$

where q_i is the vertical slowness $q_i = \cos(\theta_i)/v_i$ in the i-th layer and Δz_i is the layer thickness $\Delta z_i = z_{i+1} - z_i$. The superscripts ^{d} and ^{u} denote the downgoing (P-wave mode) and upgoing (S-wave mode) legs of the raypath in Figure 1, respectively.

To understand the τ contribution of the S-wave near-surface velocities to the total intercept time we expand the first two terms of the upgoing contribution,

$$\tau^u = \sum_{i=2}^{n-1} \Delta z_i q_i^u + (z_2 - z_1)\, q_1^u + (z_1 - z_0)\, q_0^u, \tag{2}$$

Assuming the measurement surface z_0 is at depth $z_0 = 0$ m and re-arranging terms we can write,

$$\tau^u = \sum_{i=2}^{n-1} \Delta z_i q_i^u + z_2 q_1^u + z_1 \left(q_0^u - q_1^u\right). \tag{3}$$

The first term in equation 3 provides the total upgoing τ-contribution from the conversion point up to the base of the second layer. The second term represents the contribution from the base of the second layer up to the surface with velocity v_1 and raypath angle θ_1, as if the layer with velocity v_0 were not present in the model. Therefore, the effect of the near-surface layer with velocity v_0 and thickness z_1 is contained in the last term.

To remove the S-wave traveltime effects of the near-surface we must then apply a correction of the form,

$$\Delta\tau_{NS}^u = z_1 \left(q_1^u - q_0^u\right). \tag{4}$$

Notice that in equation 4, the τ contribution of the near-surface layer ($z_1 q_0$) is removed and replaced by the τ contribution obtained with the rayparameter controlling the propagation in medium 1. Since the correction is done in terms of rayparameter values, not only the velocities, but also the propagation angles in each medium are considered in the correction. Therefore, raypath consistency can be achieved by using equation 4 to remove near surface effects.

The vertical slowness q is related to the rayparameter value by:

$$q_i^2 + p_i^2 = s_i^2, \tag{5}$$

where s_i is the total slowness ($s_i = 1/v_i$) in the i-th layer. The receiver-side near-surface correction for the intercept times can be parametrized in term of the slownesses p and s as,

$$\Delta\tau^u = z_1 \left(\sqrt{s_1^2 - p^2} - \sqrt{s_0^2 - p^2} \right). \tag{6}$$

Since the rayparameter value is constant in a horizontally layered medium, equation 6 shows that the delays introduced by the near-surface are constant for a fixed p-value, regardless of the event depth.

Dipping near-surface layer

For dipping interfaces equation 1 still holds (Diebold and Stoffa, 1981). However, the rayparameter value p is no longer constant, and its computation requires us to consider the dip of each interface.

Assuming that the effect of the near-surface on the P-wave leg has been removed and that the rest of the interfaces are flat, the vertical slowness in the near-surface layer can be computed as,

$$q_0^u = q_a \cos\phi - p_a \sin\phi. \tag{7}$$

where the apparent horizontal slowness (p_a) along the base of the near-surface layer with dip angle ϕ is given by

$$p_a = p \cos\phi - q_1 \sin\phi. \tag{8}$$

and the apparent vertical slowness (q_a) is,

$$q_a = \sqrt{s_0^2 - p_a^2}. \tag{9}$$

Equation 7 can be used to compute the vertical slownesses needed to obtain the near-surface correction in equation 4. Because the correction is still raypath-consistent a constant correction will remove the near-surface effect from all the events even if the base of the near-surface is dipping.

Relationship with interferometric near-surface corrections

The interferometric processing of near-surface corrections proposed by Henley (2012) and extended by Cova et al. (2014) to the τ-p domain relies on the crosscorrelation between

input traces and a set of pilot traces. The latter ones are meant to approximate the recorded wavefield conditions as if the near-surface velocity anomalies had not been present. Therefore, the τ differences captured by the crosscorrelation functions represent the subtraction of the input traces traveltimes and the reference (pilot) traces. Using equation 1 and assuming that the downgoing τ contributions are the same, this difference can be written as:

$$\Delta\tau_{xcorr} = \tau - \tau_{ref}. \tag{10}$$

Using equation 3 and assuming that only the depth and vertical slowness of the near-surface layer have changed we can write,

$$\Delta\tau_{xcorr} = z_1 \left(q_0 - q_1\right) - z_{1,ref} \left(q_{0,ref} - q_1\right). \tag{11}$$

Therefore, the τ difference captured by the crosscorrelation operation contains the near-surface correction at the reference conditions and the current conditions,

$$\Delta\tau_{xcorr} = \Delta\tau_{NS,ref} - \Delta\tau_{NS} \tag{12}$$

If the reference conditions at a receiver location are known then the near-surface effects can be computed from the τ differences captured by the crosscorrelation operation. In the next section we show how this can be done using a quasi-Newton inversion method.

INVERSION OF τ DIFFERENCES

To invert for the near-surface parameters we tried a quasi-Newton inversion approach. In this kind of inversion an initial guess for the model parameters is iteratively updated until the minimum of an objective function is reached. The objective function ($\Phi(\mathrm{m})$) we used here was the L_2 norm of the data misfit ($\delta\mathrm{d}$) given by,

$$\Phi(\mathrm{m}) = ||\delta\mathrm{d}||^2 = ||\mathrm{g}(\mathrm{m}) - \mathrm{d_{obs}}||^2, \tag{13}$$

where $\mathrm{d_{obs}}$ is the observed data and $\mathrm{g}(\mathrm{m})$ is the forward modelled data for a given set of model parameters m.

At each iteration i, the model parameters are updated as follows:

$$\mathrm{m_i} = \mathrm{m_{i-1}} + \delta\mathrm{m_i}, \tag{14}$$

where the model update ($\delta\mathrm{m}$) is given by,

$$\delta\mathrm{m} = \left[\mathrm{J}(\mathrm{m})^\dagger \mathrm{J}(\mathrm{m}) + \mu^2 \mathrm{I}\right]^{-1} \mathrm{J}(\mathrm{m})^\dagger \delta\mathrm{d}. \tag{15}$$

Here, μ is a regularization weight, I is the identity matrix, (†) denotes the transpose operator and $\mathrm{J}(\mathrm{m})$ is the Jacobian or sensitivity matrix, with elements:

$$\mathrm{J}(\mathrm{m}) = \left[\frac{\partial \mathrm{g}(\mathrm{m})}{\partial \mathrm{m}}\right]. \tag{16}$$

In our inversion problem there are four parameters we need to solve for $(z, s_0, s_1, \phi,)$. Thus, the terms in the sensitivity matrix are,

$$\mathrm{J(m)} = \left[\frac{\partial \mathrm{g(m)}}{\partial \mathrm{z}}, \quad \frac{\partial \mathrm{g(m)}}{\partial \mathrm{s_0}}, \quad \frac{\partial \mathrm{g(m)}}{\partial \mathrm{s_1}}, \quad \frac{\partial \mathrm{g(m)}}{\partial \phi}\right]. \tag{17}$$

Using the formulae developed in the previous section we can write each one of the derivatives in 17 as,

$$\frac{\partial \Delta\tau}{\partial z} = (q_0 - q_1) \tag{18}$$

$$\frac{\partial \Delta\tau}{\partial s_0} = \frac{z s_0}{q_a}\cos(\phi) \tag{19}$$

$$\frac{\partial \Delta\tau}{\partial s_1} = \frac{z s_1}{q_1}\cos^2(\phi)\left(\tan(\phi)\frac{p_a}{q_a} - 1\right) \tag{20}$$

$$\frac{\partial \Delta\tau}{\partial \phi} = z(p'_a - q_a)\left[\frac{p_a}{q_a}\cos(\phi) + \sin(\phi)\right] \tag{21}$$

with,

$$p'_a = p\sin(\phi) + q_1\cos(\phi) \tag{22}$$

The inversion algorithm is stopped once a given number of iterations is reached or when a given threshold for the objective function is achieved.

SYNTHETIC DATA TESTS

To test this inversion approach we first used equation 11 to compute the τ differences at each one of the receiver locations in the near-surface model shown in Figure 2a. Figure 2b shows the τ differences that would be obtained at three different receiver locations using the near-surface parameters at $x = 1800$m as the reference parameters. Notice how the shape of the τ differences are controlled by the geometry of the near-surface base.

Using the formulae developed in the previous section we inverted the data at each receiver location. Figure 3 shows the results both in model space and data space. We used a smoothed version of the actual near-surface structure as our initial guess for the depth parameter. The initial v_0 and v_1 values were set at 400m/s and 600m/s respectively. The initial dip values were computed from the initial depth model. All these parameters are represented as dashed lines on Figure 3a. There, the results show that all the true parameters of the model were successfully recovered at each receiver location. Figure 3b compares the data computed with our initial parameters and the data modelled with the true and inverted near-surface parameters. The results show how the inversion succeeded in finding the model parameters that reproduce the input data.

To approximate our experiment to conditions similar to the ones expected on field data, we added uniformly distributed random noise between -0.1ms and 0.1ms to the previously generated τ differences. The results of the inversion with these data are shown in Figure 4. Notice that despite the data modelled after the inversion seems to match the input data

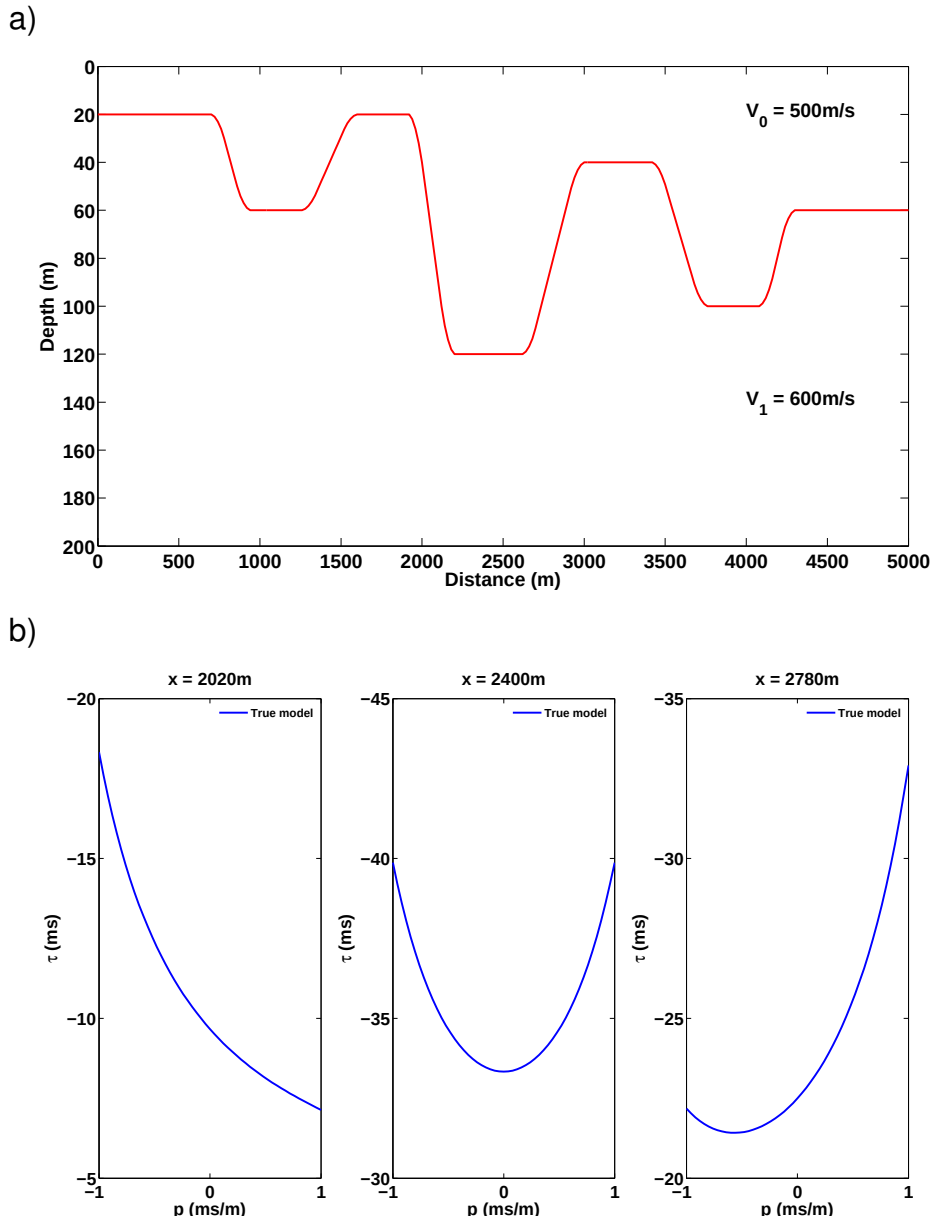

FIG. 2. a) Near-surface velocity model used to test the inversion. b) τ differences modelled at three different x-locations

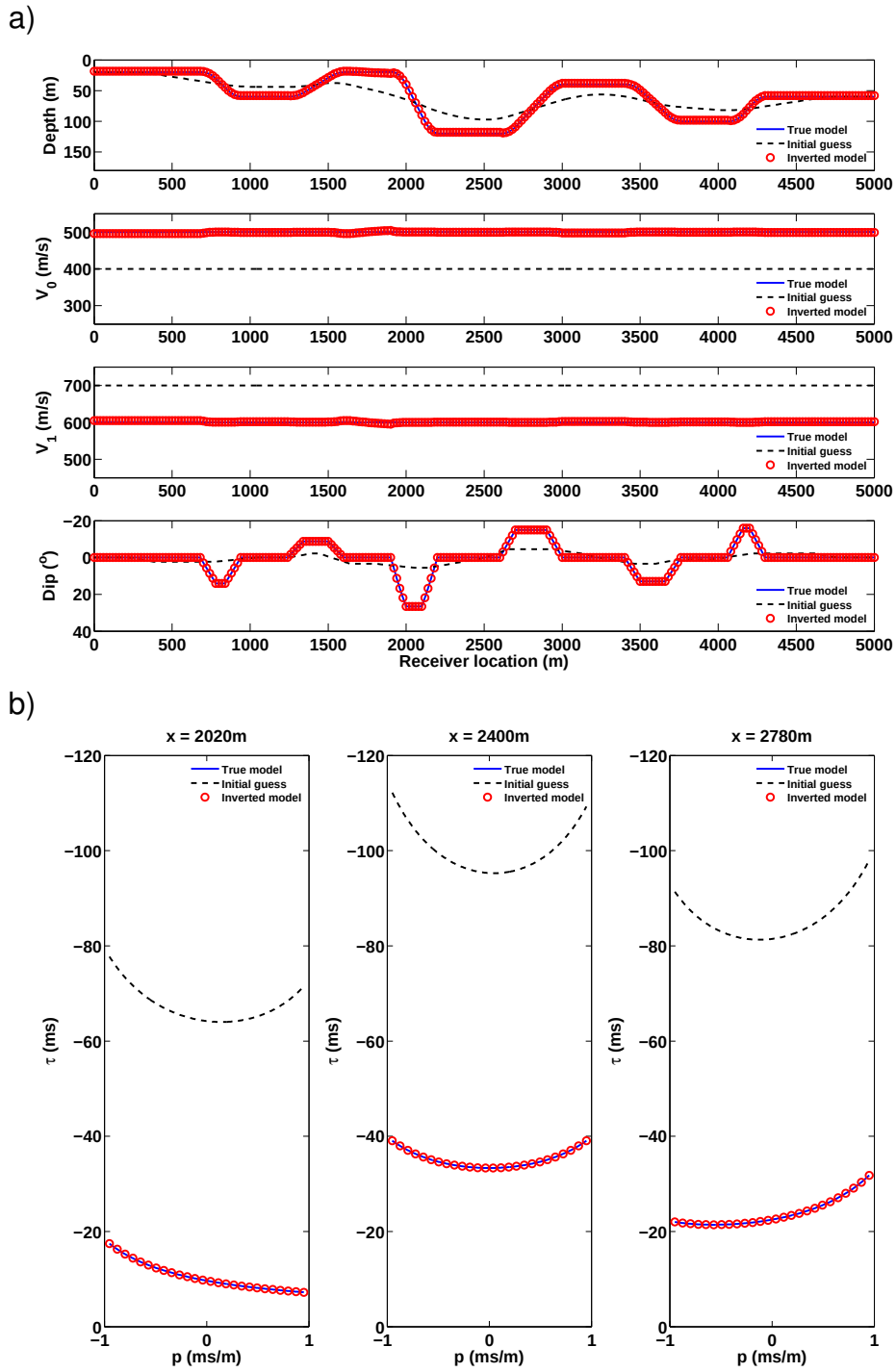

FIG. 3. Inversion results in a) model space and b) data space.

reasonably well (Figure 4a) the inverted depth and velocities in Figure 4b display unstable results. This contrasts with the inverted dip values which show a very good match with the true values.

In addition to adding noise to the data we also studied the effect of using a limited range of p values for the inversion. For this, we ran the inversion using only the data between -0.5ms/m and 0.5ms/m. The results displayed on Figure 5 are very similar to the ones obtained in the previous test. However, we noticed that the inverted depth values are closer to the initial depth model. Also, the inverted velocity values seems more stable than in the previous test. Despite the fact that the inverted dips are slightly noisier, the results are reasonably stable.

In an attempt to stabilize the inversion we increased the value of the regularization weight from 0.01 to 0.1. The results are shown in Figure 6. In general, these results are more stable. Inverted velocities are stable and close to the true velocities. However, inverted depth values are more constrained around the initial guess and still far from the true values. On the other hand, the inverted dips matched the true dip values, confirming the robustness of the inversion of this parameter.

Raytraced data tests

To further test the inversion we also computed synthetic traces via raytracing using the same near-surface velocity model as before but including five additional horizontal interfaces (Figure 7). Notice that no P-wave velocity contrast exists between the near-surface layer and the medium beneath to simulate the data as if P-wave statics were already removed. Also, only PS-traveltimes were modelled during the raytracing, no amplitude variations were included.

Figure 8 displays the data recorded at $x = 2500$m in three different domains. Notice how in the shot gather domain, receiver-side near-surface effects distort the moveout of the events. After sorting the data into common receiver gathers the data do not display major moveout distortions. This helps to obtain a very clean and coherent transformation to the τ-p domain.

Figure 9 shows the crosscorrelation between the τ-p gather obtained at the reference location A ($x = 1800$m) and the current location B ($x = 2020$m). Notice how the modelled differences using equation 11 and the picked maximum of the crosscorrelation traces match really well. Figure 10 compares the picked and modelled differences for three different locations. Despite the presence of a few outliers the τ differences match really well. These outliers are the result of numerical artifacts being introduced by the limited aperture (offsets) used during the τ-p transformation. These artifacts distort the location of the maximum of the crosscorrelation functions at very specific p-values. On the rest of the data no major interference was identified.

Figure 11 displays the results obtained using the raytraced data. The regularization parameter was set at 0.1, since it provided the most stable results. These results are very similar to the ones obtained in the previous section. Inverted depth values for the near-

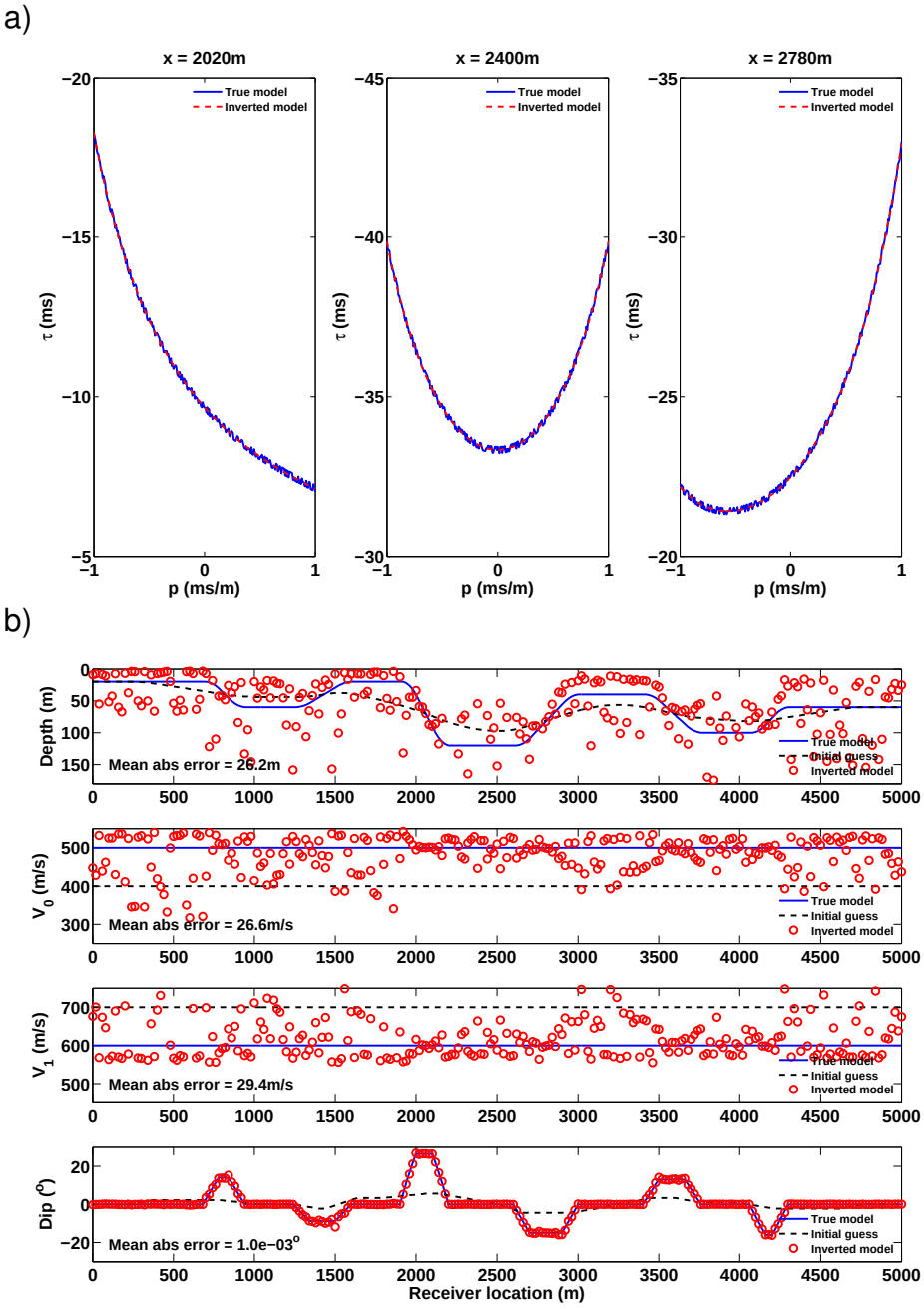

FIG. 4. Results after inverting noisy data. a) Input and modelled data after inversion. b) Inverted parameters.

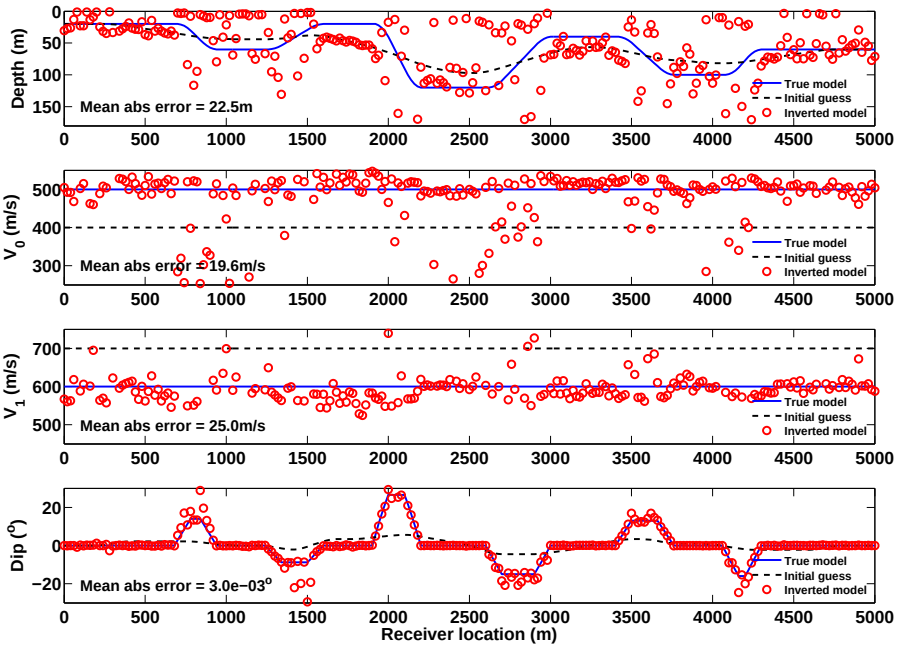

FIG. 5. Inversion results after using only the data between -0.5ms/m and 0.5ms/m.

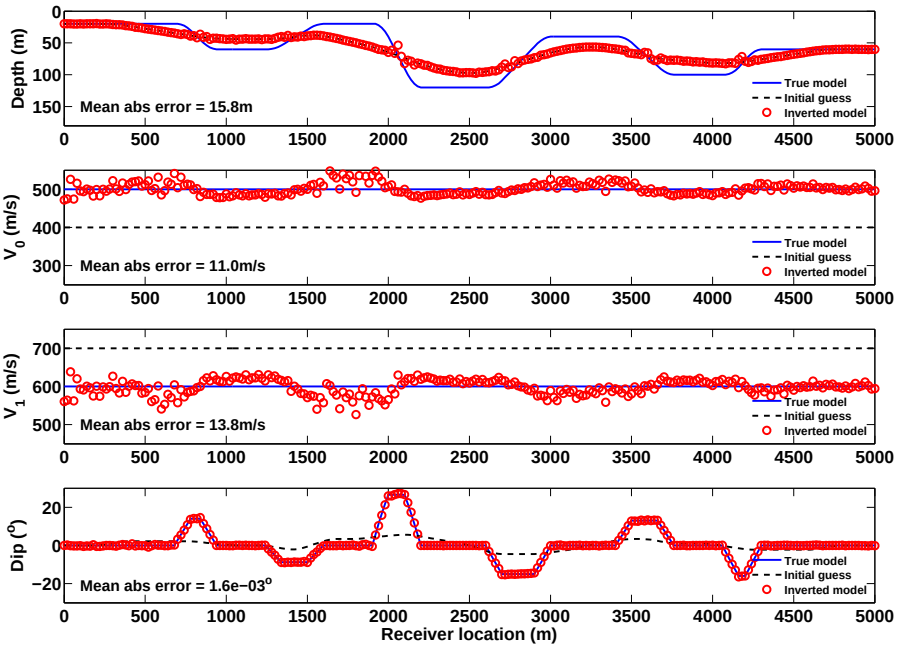

FIG. 6. Inversion results after increasing regularization weight from 0.01 to 0.1.

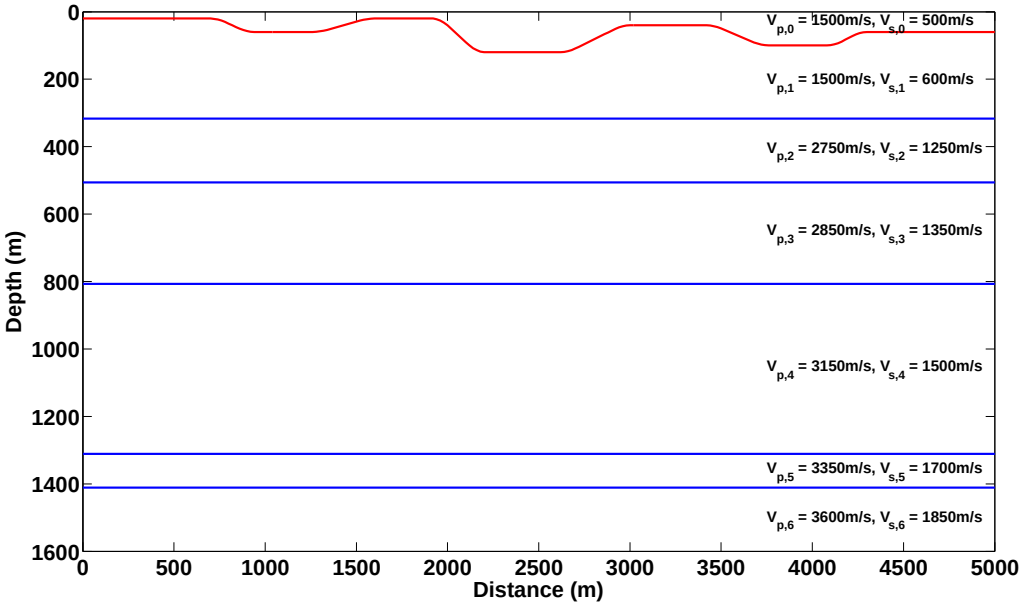

FIG. 7. Velocity model used to compute synthetic converted-wave traces via ray-tracing.

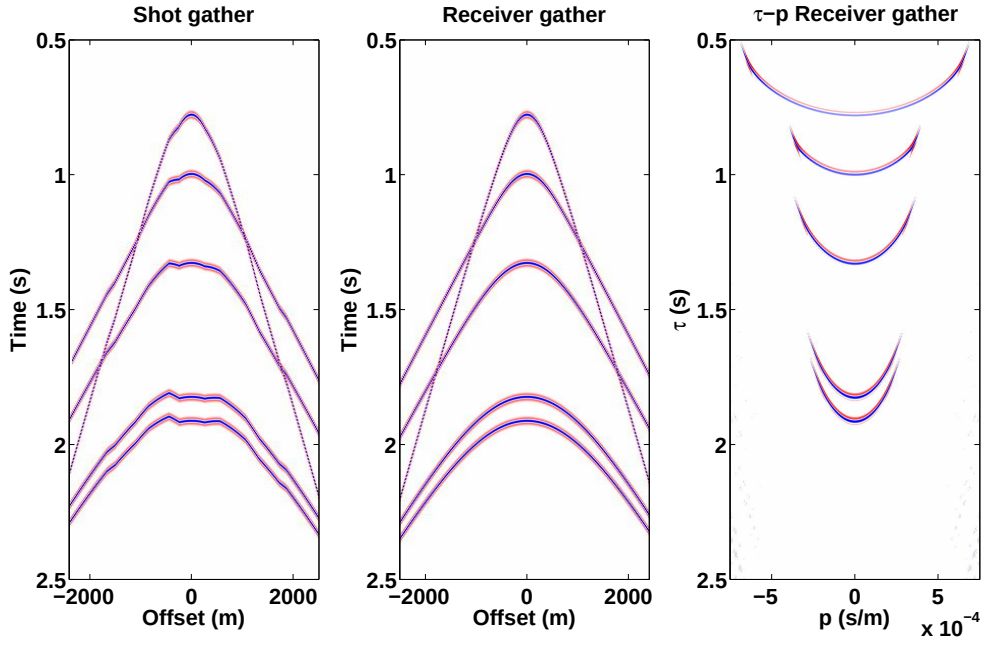

FIG. 8. Raytraced data recorded at x =2500m on three different domains.

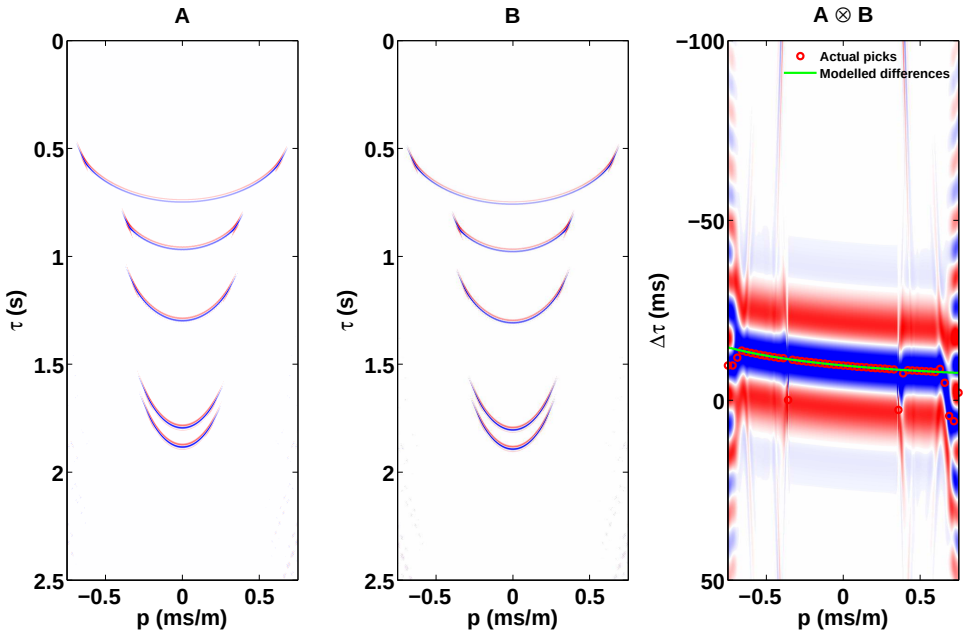

FIG. 9. Crosscorrelation between reference τ-p gather (A) and τ-p data at receiver location x =2020m (B). Modelled and picked τ differences are overlaid on the crosscorrelation panel .

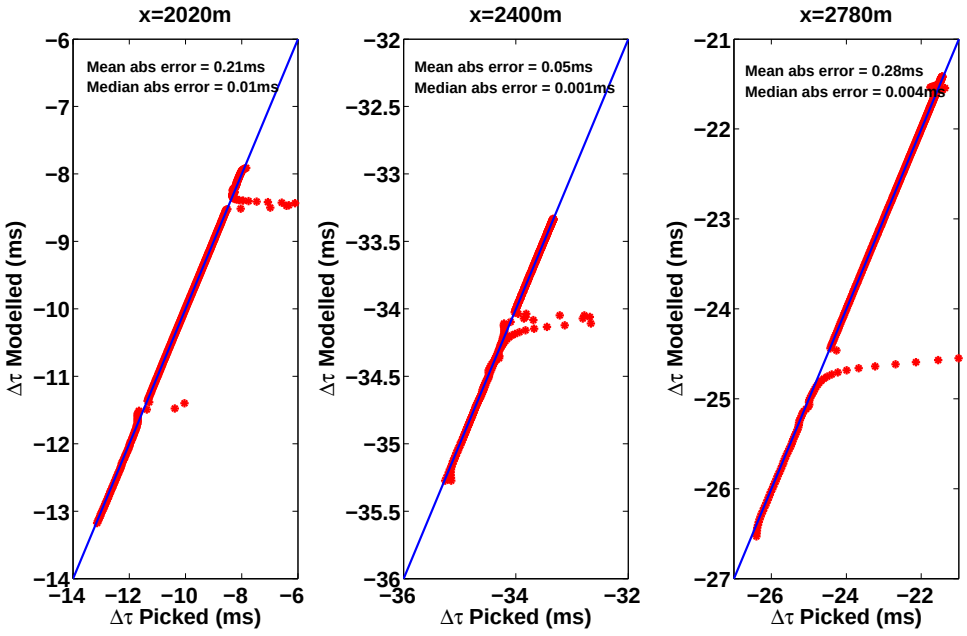

FIG. 10. Comparison between modelled and picked τ differences at three different receiver locations

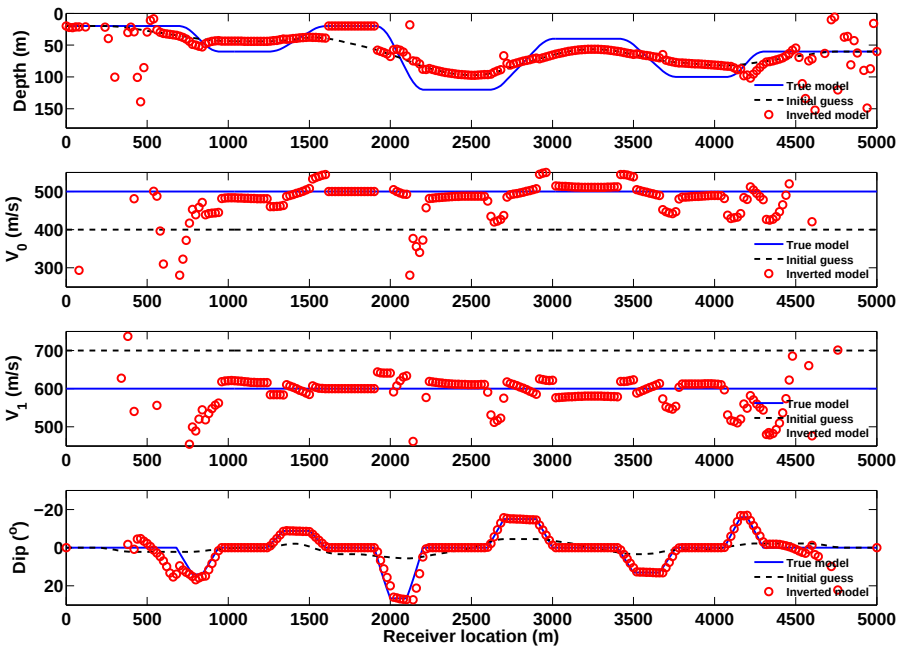

FIG. 11. Inversion results obtained using the raytraced data.

surface layers seems to be very constrained around the initial depth model. However, the inverted velocity values are close to the actual velocities. Moreover, the inverted dips again display very good and stable results.

CONCLUSIONS

The inversion presented in this study is an alternative to conventional methods for computing S-wave velocities in the near-surface using converted-wave data. Our approach requires that the near-surface parameters at one reference location be known. Therefore, any result provided by the inversion will depend of the accuracy of this information.

In all our tests the depth of the near-surface base was the most difficult parameter to invert for. The presence of noise in the picks or the lack of a wide range of p-values had an important effect on the stability of the inversion. The inverted velocities were also affected by these limitations although to a lesser degree.

The inverted dips displayed by far the most stable results. Since this parameter controls the shape of the data, it is less sensitive to errors in the individual picks. Based on this observation a different parametrization of the inversion problem using the inverted dips as a constraint might be a good alternative for improving the inversion of the rest of the parameters. Also, since the structure of the near-surface at a given location must be know, the depth of this layer can be mapped by projecting the known depth using the inverted dips.

Different parameterizations and inversion methods should be explored to improve the results for this study. Application of this method on real datasets remains to be explored.

ACKNOWLEDGEMENTS

The authors thank the sponsors of CREWES for continued support. This work was funded by CREWES industrial sponsors and NSERC (Natural Science and Engineering Research Council of Canada) through the grant CRDPJ 461179-13. We also thank David Henley for his suggestions and assistance with proof-reading.

REFERENCES

Cova, R., Henley, D., and Innanen, K., 2014, Addressing non-stationary shear wave statics in the rayparameter domain: CREWES Research Report, **26**, 1–17.

Diebold, J. B., and Stoffa, P. L., 1981, The traveltime equation, tau-p mapping, and inversion of common midpoint data: Geophysics, **46**, No. 3, 238–254.

Henley, D., 2012, Interferometric application of static corrections: Geophysics, **77**, No. 1, Q1–Q13.